Materials Research. 2017; 20(Suppl. 2): 694-700
DOI: http://dx.doi.org/10.1590/1980-5373-MR-2016-0929

A Microrheological Study of Poly(Methyl Methacrylate) Elastomer/Poly(Ethylene Terephthalate) ($PMMA_{elast}$/PET) Blends

Juciklécia da Silva Reinaldo[a], Igor Zumba Damasceno[c], Marcelo Massayoshi Ueki[b], Edson Noriyuki Ito[c]*

[a]Programa de Pós-Graduação em Ciência e Engenharia de Materiais (PPgCEM), Universidade Federal do Rio Grande do Norte (UFRN), Natal, RN, Brazil
[b]Departamento de Ciência e Engenharia de Materiais (DCEM), Universidade Federal de Sergipe (UFS), São Cristóvão, SE, Brazil
[c]Departamento de Engenharia de Materiais (DEMat), Universidade Federal do Rio Grande do Norte (UFRN), Natal, RN, Brazil

Received: December 06, 2016; Revised: September 04, 2017; Accepted: October 27, 2017

This study involved an evaluation of the influence of phase inversion in poly(methyl methacrylate) elastomer/poly(ethylene terephthalate) binary blends ($PMMA_{elast}$/PET) and the effect of the addition of poly(methyl methacrylate-glycidyl methacrylate-ethyl acrylate) (MGE) interfacial compatibilizer on the microrheological properties of this polymer blend. Thermal, dynamic mechanical thermal, rheological and morphological analyses were performed using sensitive techniques such as differential scanning calorimetry (DSC), dynamic mechanical thermal analysis (DMTA), parallel plates rheometry in the linear viscoelastic region, and atomic force microscopy (AFM), respectively. In this study, it was found that variations in the percentage of the PET phase influenced the correlation between the rheological properties at low shear rates and the morphology of the $PMMA_{elast}$/PET binary blend and of the $PMMA_{elast}$/PET/MGE compatibilized blend.

Keywords: *PMMA/PET blend, parallel plates rheometry, AFM.*

1. Introduction

PMMA/PET blends are used in electrical and automotive applications which require materials with good dimensional stability, mainly for electronic circuits. However, these polymer blends are immiscible and incompatible[1-4] so they require the addition of an interfacial compatibilizer to improve the dispersion of the dispersed phase, thereby reducing the interfacial tension, stabilizing the morphology by reducing coalescence, and improving the interfacial adhesion between the phases[5,6].

The purpose of using a compatibilizer in immiscible polymer blends is to improve their final properties, and several analytical methods should therefore be employed to verify the efficiency of interfacial compatibilization. Microscopic characterizations by transmission electron microscopy (TEM), scanning electron microscopy (SEM) and atomic force microscopy (AFM) can provide evidence of the efficiency of compatibilization in polymer blends. Other characterization techniques such as rheological studies using low shear rates in the linear viscoelastic region of melt polymers can be used to complement the results obtained in the evaluation of possible changes in the rheological behavior of molten compatibilized polymer blends[7].

Several authors, cited below, report the effect of compatibilization on the morphology and rheology of immiscible polymer blends compatibilized with MGE terpolymer, composed of methyl methacrylate (MMA), glycidyl methacrylate (GMA) and ethyl acrylate (EA). In studies using MGE terpolymer as a compatibilizer for PBT/ABS, PBT/AES and PBT/SAN blends [8-12], it was found that the GMA epoxy group can react with the PBT terminal groups and may lead to the formation of a copolymer (PBT-*g*-MGE) at the interface of these polymer blends during the melt processing, which will alter their final properties.

Larocca et al.[10], who examined the efficiency of the reactive compatibilization of MGE on the properties of PBT/AES blends, found that the formation of PBT-*g*-MGE copolymer at the interface of these blends altered their morphological and rheological properties. These effects became more intense in response to an increase in the overall concentration of GMA (present in the composition of the MGE) in the blend and to a reduction in the molecular weight of MGE. Costa et al.[11] carried out a study on SAN/PBT blends compatibilized with MGE, and reported that an analysis by TEM revealed a significant reduction in the dispersed phase of PBT in response to the addition of MGE, thus demonstrating the reaction efficiency of MGE with the final groups of PBT chains due to the *in situ* reactions that occurred during processing.

*e-mail: ito@ufrnet.br

MGE terpolymer has also proved to be an excellent compatibilizer in PMMA/PET blends, since PET chain ends have the same carboxyl and hydroxyl groups, which are similar to those found in PBT. In this studies[12], TEM and AFM analyses revealed that increasing the percentage of molecular weight of PET in the PMMA/PET binary blend led to a significant increase in the mean diameters of the dispersed phase. Conversely, the use of MGE in these blends reduced the mean diameters of the dispersed phase in compositions containing the same percentage of PET of the binary blend.

Poly (methyl methacrylate) with elastomeric particles ($PMMA_{elast}$)[13,14] and PET have complementary properties[15]; hence, variations in the composition of their mixtures alter their structural and morphological characteristics. Earlier studies of $PMMA_{elast}$/PET immiscible polymer blends conducted by Reinaldo et al.[16] revealed synergistic properties that can be used in specific applications. As for the efficiency of compatibilization, the authors found evidence of dual reactivity between MGE and PET, and also with $PMMA_{elast}$, due to the presence of the elastomer phase of PMMA.

In studies of the morphology of immiscible polymer blends, rheological characterization is extremely important because it sheds light on the final properties of these blends[17-19], especially in polymer blends with complex morphologies constituted by copolymers with elastomeric particles, such as the $PMMA_{elast}$ contained in $PMMA_{elast}$/PET blends. Therefore, our goal was to perform a microrheological study of $PMMA_{elast}$/PET blends with and without the use of an interfacial compatibilizer, MGE, up to phase inversion, using parallel plates rheometry and atomic force microscopy.

2. Materials and Methods

2.1 Materials

The materials used in this work were PMMA copolymerized with elastomeric particles ($PMMA_{elast}$) (ECP800) (MFI = 3. 8 g/10 min, ASTM D 1238[21], 230ºC/2.16 kg, according to the manufacturer) produced by Unigel S.A. and PET from soft drink bottles (MFI = 15 g/10 min, ASTM D 1238[21], 250ºC/2.16 kg, according to the authors). The interfacial compatibilizer used here was poly(methyl methacrylate-glycidyl methacrylate-ethyl acrylate) (MGE) terpolymer with a composition of: 88 wt% methyl methacrylate, 10 wt% glycidyl methacrylate and 2 wt% ethyl acrylate, which was synthesized in the laboratory as described in the literature[9,20].

2.2 Extrusion mixing and injection molding

The $PMMA_{elast}$/PET binary blend up to phase inversion and the compatibilized $PMMA_{elast}$/PET/MGE blend were processed in a co-rotating twin screw extruder (D = 16 mm and L/D=40) under the following processing conditions: temperature profile of 102/160/190/210/220/230/220/210ºC; feed speed of 80 rpm; and screw speed of 220 rpm. After extrusion, the pure polymers and the polymer blends were granulated and dried at 60ºC in a vacuum oven for 12 hours. These materials were then molded (ASTM standard D638[22]) in an Arburg 270V injection molding machine using a temperature profile of 230/240/240/250/250ºC, mold temperature of 50ºC and a cooling time of 50 s. The injection molded test specimens were used for the thermal, dynamic mechanical thermal, rheological and morphological analyses.

2.3 Thermal characterization by Differential Scanning Calorimetry (DSC) and Dynamic Mechanical Thermal Analysis (DMTA)

The DSC analyses were performed in a Netzsch DSC 200 F3 Maia differential scanning calorimeter using about 6 mg of sample, which was placed in an aluminum crucible and subjected to the following conditions: nitrogen atmosphere at a flow rate of 50 $mL \cdot min^{-1}$ and a heating rate of $10ºC \cdot min^{-1}$ from 20 to 290ºC. The DMTA analyses were carried out in an Anton Paar parallel plates rheometer equipped with a SRF 12 accessory in torsion at a frequency of 1 Hz and the temperature ranged from 20 to 130ºC at a scanning rate of $2ºC \cdot min^{-1}$.

2.4 Rheological characterization by parallel plates rheometry

The rheological analyses of the pure polymers and the $PMMA_{elast}$/PET and $PMMA_{elast}$/PET/MGE blends were carried out in the linear viscoelastic region, using an Anton Paar MCR 302 parallel plates rheometer, at a temperature of 270ºC in the frequency range of 1000 to 0.01 $rad \cdot s^{-1}$.

2.5 Morphological characterization by Atomic Force Microscopy (AFM)

Samples taken from the injection molded test specimens were first trimmed and then cut into ultra-thin sections in a RMC Power Tome-X Cryo-Ultramicrotome, using a Diatome Diamond Cryo Histo 45º knife, with sample temperature at -80ºC, knife temperature at -60ºC, liquid nitrogen cooling, cutting speed of 0.2 $mm \cdot s^{-1}$, and final section thickness of 25 nm. The morphological analysis was performed via non-contact atomic force microscopy, using a Shimadzu SPM-9700 microscope at a frequency of 1 Hz.

3. Results and Discussion

3.1 Thermal Characterization by Differential Scanning Calorimetry (DSC) and by Dynamic Mechanical Thermal Analysis (DMTA)

Thermal characterizations were performed by DSC and DMTA to evaluate the parameters that affect processability and the effects of the MGE compatibilizer on the $PMMA_{elast}$/

PET blends. The DSC curves shown in Figure 1, and their values listed in Table 1, indicate that the behavior of $PMMA_{elast}$ is typical of an amorphous polymer, showing only the PMMA glass transition temperature (T_g = 94.4ºC), because the T_g of the elastomeric phase was not measured by this technique (the start of test temperature was above ambient temperature). While PET, a semicrystalline polymer, presented a glass transition temperature (T_g = 70.4ºC), a crystallization temperature (T_c = 121.2ºC) and a crystalline melting temperature (T_m = 254ºC). The $PMMA_{elast}$/PET blends exhibited clear thermal transition temperatures (Figure 1), except for the blend containing 15 wt% of PET phase (see Table 1) that could not be quantified using this technique.

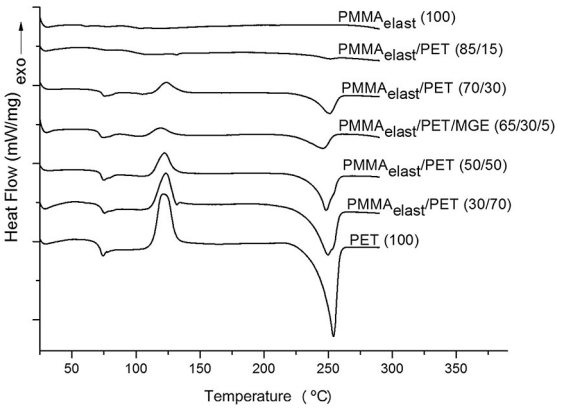

Figure 1. DSC curves of the pure polymers and the $PMMA_{elast}$/PET and $PMMA_{elast}$/PET/MGE blends.

The DSC results also indicated the reactive compatibilization obtained with MGE was effective, based on signs of a decrease in crystalline phase in the blend containing 30 wt% of PET in response to this interfacial compatibilizer. The binary blend $PMMA_{elast}$/PET contained 26.5 wt% of crystalline phase (PET) and the compatibilized blend $PMMA_{elast}$/PET/MGE had 24.7 wt% of crystalline phase, as can be seen in Table 1. This decrease in the crystallinity of polymer blends in the same composition using a reactive compatibilizer has been reported by other researchers[10], who attributed it to phase anchoring and increased molecular weight due to the reaction between the interfacial compatibilizer and the semicrystalline polymer.

Although the crystalline melting temperature of the $PMMA_{elast}$/PET binary blend is lower than the pure PET, it did not vary as a function of increased of molecular weight percentage up to the phase inversion of the binary blend. Given the reactivity of the epoxy group of MGE with the chain ends of PET and also with the elastomeric phase of PMMA[14] significantly reduces the crystalline melting temperature of PET in the $PMMA_{elast}$/PET/MGE blend.

The DMTA results shown in Figure 2 pertain to the glass transition temperature (T_g) of pure PET, pure PMMA and the PMMA in the $PMMA_{elast}$/PET blend. The T_g of the elastomeric phase was not measured by this technique (the start of test temperature was above ambient temperature) and the T_g of the PET in the $PMMA_{elast}$/PET blends was not measured due to overlapping with the T_g peak of the PMMA.

The α-relaxations pertaining to the glass transition temperatures of the polymers can be observed by means of the tan δ peak, i.e., the highest characteristic value of the tan δ peak corresponds to the material's glass transition temperature[23]. Figure 2 shows that the differences in the tan δ peak values of $PMMA_{elast}$ and PET are related to the different values of the glass transition temperatures (T_g) of these polymers. Because PMMA is an amorphous polymer, its peak was higher than that of PET, which is a semicrystalline polymer. As for the $PMMA_{elast}$/PET blends, the curves of the compositions showed a shift in the T_g of PMMA in response to the increase in the proportion of PET.

3.2 Microrheology of the $PMMA_{elast}$/PET and $PMMA_{elast}$/PET/MGE blends

Figure 3 correlates the morphological results obtained by AFM with the rheological results of the storage modulus (G') versus the loss modulus (G") of the pure polymers and the $PMMA_{elast}$/PET binary blend as a function of the variation in the dispersed phase of PET. A significant difference was found in the values of the G' vs. G" curves of $PMMA_{elast}$ and PET, because $PMMA_{elast}$ is a copolymer that contains an elastomeric phase and PET is a homopolymer. Changes

Table 1. Thermal transitions and percent crystallinity of the pure polymers and the $PMMA_{elast}$/PET and $PMMA_{elast}$/PET/MGE blends

Compositions (wt%)	T_g^{PMMA} (ºC)	T_g^{PET} (ºC)	T_{cc} (ºC)	ΔH_{cc} (J/g)	T_m (ºC)	ΔH_m (J/g)	x_c (%)
$PMMA_{elast}$ (100)	94.4	-	-	-	-	-	-
$PMMA_{elast}$/PET (85/15)	87.2	64.0	-	-	252.0	0.92	4.4
$PMMA_{elast}$/PET (70/30)	103.4	72.3	123.7	5.83	251.4	11.14	26.5
$PMMA_{elast}$/PET/MGE (65/30/5)	119.1	69.8	119.1	4.10	246.3	10.36	24.7
$PMMA_{elast}$/PET (50/50)	103.1	71.5	122.4	10.05	251.7	18.92	27.0
$PMMA_{elast}$/PET (30/70)	97.3	71.5	123.6	13.44	252.0	30.13	30.7
PET (100)	-	70.4	121.2	25.32	254.0	44.83	32.0

T_g^{PMMA}, T_g^{PET}, T_{cc}, T_m and ΔH_{cc}: Values related to temperatures of glass transition, crystallization, and crystallization and melting point enthalpy in the first heating cycle. Calculation of x_c according to the following equation: $x_c = \frac{\Delta H_f}{\Delta H_f^\circ} x100\% \text{ (pure PET)}$[23] $x_c = \frac{\Delta H_f}{W_{PET} x \Delta H_f^\circ} x\ 100\%$ (polymer blends)[24]. The ΔH_f° of PET is 140 (J/g)[23]

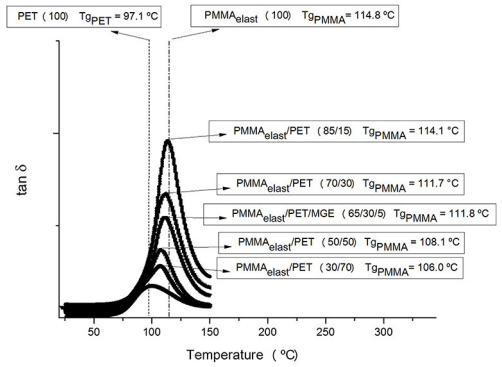

Figure 2. Tan δ curves of the pure polymers and the PMMA$_{elast}$/PET and PMMA$_{elast}$/PET/MGE blends.

in the PET content of the polymer blends caused variations in both the morphological characteristics and rheological behavior shown on the G' vs. G" curves, indicating that the addition of PET phase affects the microrheological behavior of the PMMA$_{elast}$/PET blend.

Figure 4 shows how the addition of MGE compatibilizer influences the rheological and morphological behavior when compared to the binary blends. The G'G" vs. frequency (ω) curves of the pure polymers reveal the differences in the rheological behavior of these two polymers, which are directly related to the morphology of PET (homopolymer) and of PMMA$_{elast}$ (copolymer). The presence of the elastomeric phase in the PMMA$_{elast}$ copolymer showed higher G'G" values at low frequency than the PET.

Two G' = G" crossover points were also observed, where the dissipative and elastic properties of the PMMA$_{elast}$ at 270ºC were the same at the same frequency, with G' = G" values at high frequency (ω = 160 rad/s) and low frequency (ω = 0.65 rad/s), while only one G' = G" crossover point was observed at low frequency (ω = 1 rad/s) in PET at 270ºC. The behavior of PMMA$_{elast}$ observed here is attributed to the crosslinks in rubber, which influence the rheological behavior of rubber-toughened acrylic copolymers, as has been reported by other authors[19].

The compatibilized blend with MGE, i.e., the PMMA$_{elast}$/PET/MGE blend, did not show the G' = G" crossover point on the G' G" versus ω curve, and in the low frequency region, the storage modulus (G') is much higher than the loss modulus (G"). This behavior is attributed to the chemical reactions that occur between PMMA$_{elast}$ and PET with MGE. The presence of these bonds at low shear rates causes the material to behave like a solid; hence, the value of G' is higher than the G". The reactive compatibilization of MGE with the carboxyl and hydroxyl groups of PET, and also with the elastomeric particles in PMMA$_{elast}$ copolymer, has been reported previously by Reinaldo et al.[3]. A smaller size distribution of the dispersed phase of PET was found in the PMMA$_{elast}$ matrix of the compatibilized blend than in the binary blend with the same PET content.

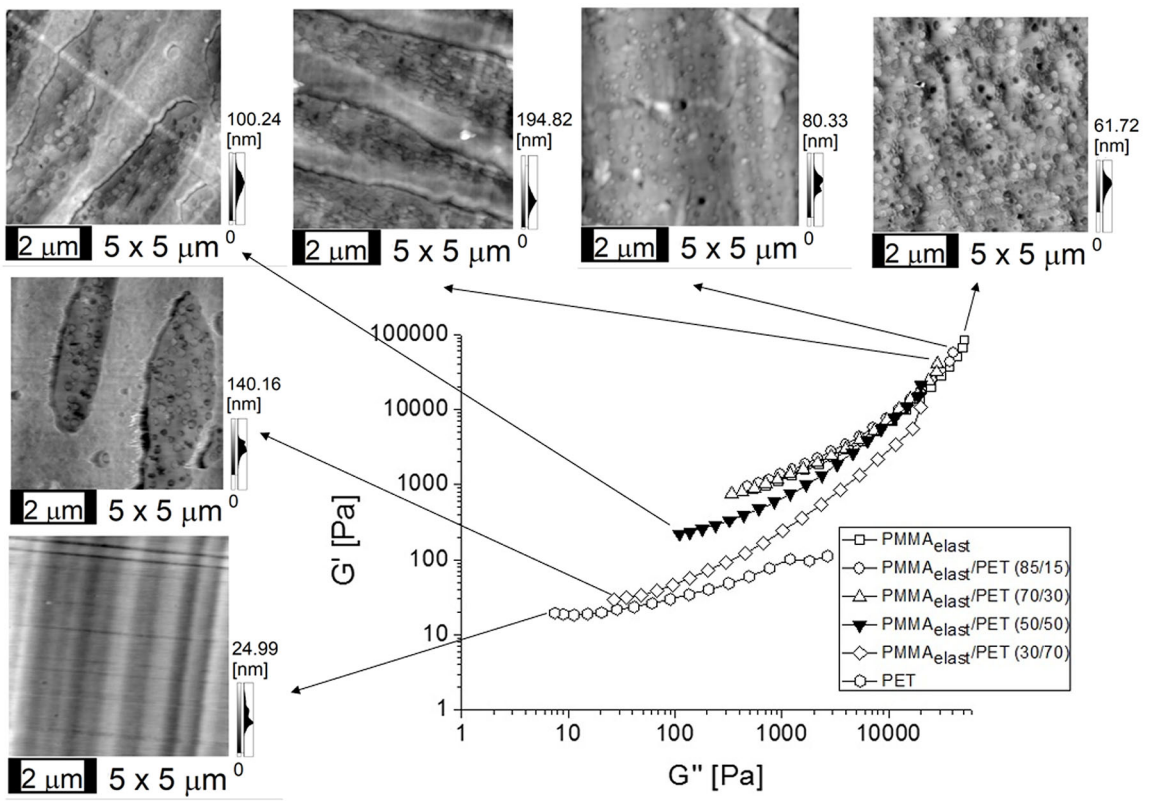

Figure 3. Correlation between the morphology and rheology of the PMMA$_{elast}$/PET binary blend at 270ºC.

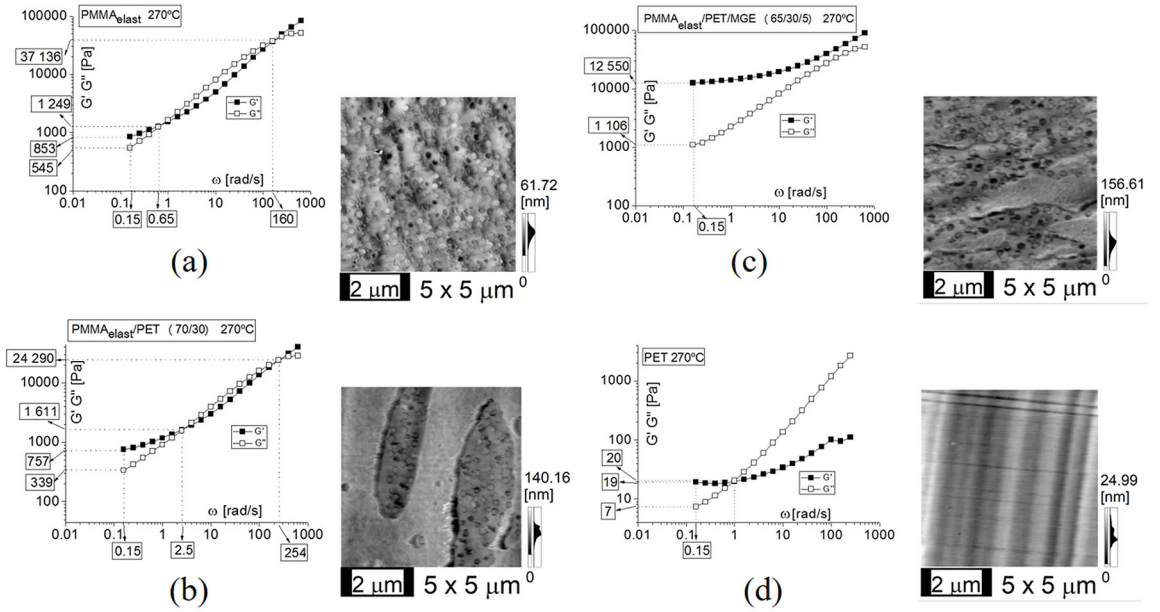

Figure 4. Correlation between rheology and morphology determined by low shear rate rheology and AFM: a) PMMA$_{elast}$ (100 wt%); b) PMMA$_{elast}$/PET blend (70/30 wt%); c) PMMA$_{elast}$/PET/MGE blend (65/30/5 wt%); d) PET (100 wt%), at 270ºC.

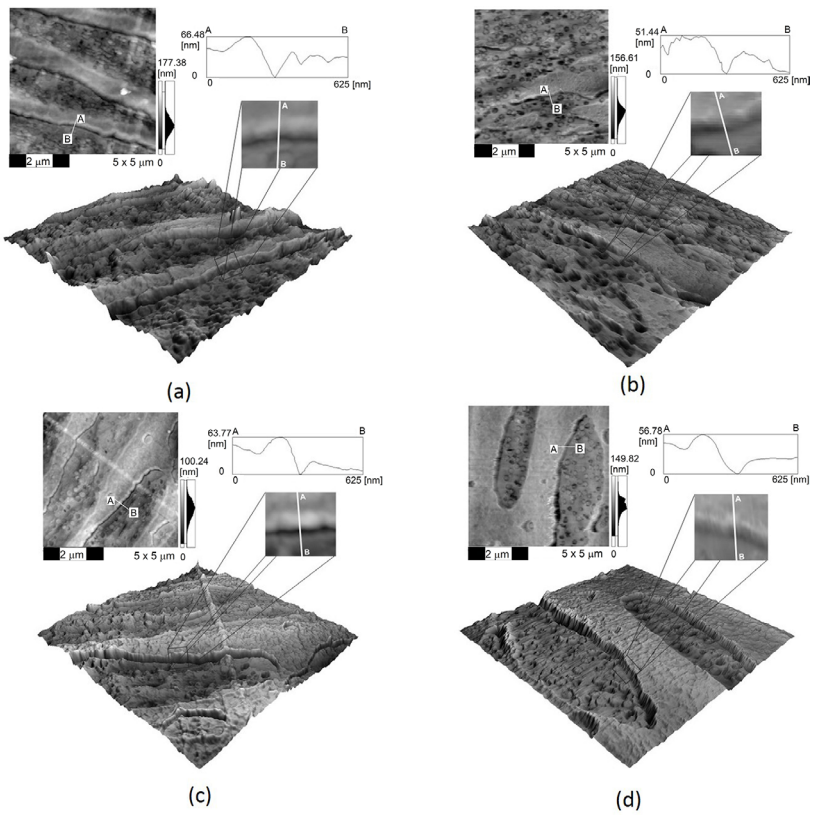

Figure 5. Interfacial analysis of the 3D morphology of the binary blend, the use of interfacial compatibilizer, and the phase inversion: a) PMMA$_{elast}$/PET blend with 30 wt% of PET; b) PMMA$_{elast}$/PET/MGE blend with 30 wt% of PET and 5 wt% of MGE; c) PMMA$_{elast}$/PET blend with 50 wt% of PET; d) PMMA$_{elast}$/PET blend with 70 wt% of PET.

Figure 5 illustrates the 3D morphology of the PMMA/PET interfacial region up to phase inversion, as well as that resulting from the use of MGE as interfacial compatibilizer in the PMMA$_{elast}$/PET/MGE blend. Sectioning the material using a diamond knife below the glass transition temperature (T_g) of the polymers was successful in cutting without structural deformations of the interface. In addition, the expansion of the phases as a function of the specific thermal expansion coefficient of each polymer allowed evaluations to be made of the differences at the interfaces of the blends as a function of phase inversion (30 to 70 wt% of PET) and the use of 5 wt% of MGE in the PMMA$_{elast}$/PET blends.

Figure 6 shows the mean values of the height of the interface between PMMA and PET in the PMMA$_{elast}$/PET blends. The interface values for the compatibilized blends with MGE were lower than those of the binary blends containing 30, 50 and 70 wt% of PET phase. Therefore, the decrease in interfacial height, which has to do with the thermal expansion coefficient, provided evidence of better phase dispersion in the PMMA$_{elast}$/PET blends in response to the use of MGE.

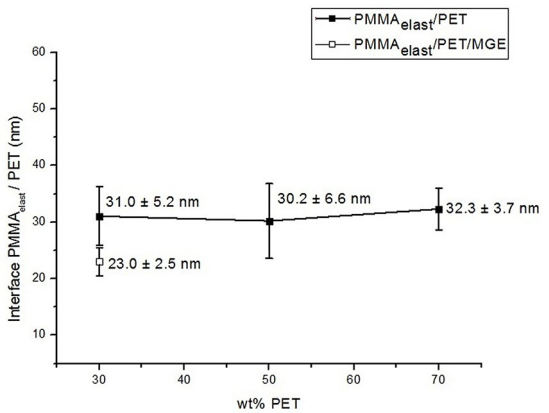

Figure 6. Measures of the difference in the interface of PMMA$_{elast}$/PET and PMMA$_{elast}$/PET/MGE blends.

Figure 7 depicts the results of complex viscosity (η*) as a function of frequency (ω) in the linear viscoelastic region of the pure polymers, the PMMA$_{elast}$/PET binary blend and the PMMA$_{elast}$/PET/MGE blend compatibilized at 270ºC. As can be seen, neither PMMA$_{elast}$ nor PET presented Newtonian behavior at low frequencies at the temperature of 270ºC.

As for the behavior of the PMMA$_{elast}$/PET blends, the findings indicate that the complex viscosity (η*) of the PMMA$_{elast}$ matrix did not change significantly in response to the addition of 15 and 30 wt% of the PET phase. Only the binary blends containing 50 and 70 wt% of PET showed such changes, and an increasing PET content should tend to bring the values close to the pure PET.

The compatibilized blend showed much higher complex viscosities (η*) at low shear rates than the pure polymers and the binary blend with the same content of PET phase (30 wt% of PET). This corroborates with the efficiency results of the dual reactive interfacial compatibilization of PMMA$_{elast}$/PET blend with MGE[16]. According to other researchers[25], the compatibilization mechanism involves the induction of interfacial interactions between the components of the polymer blend.

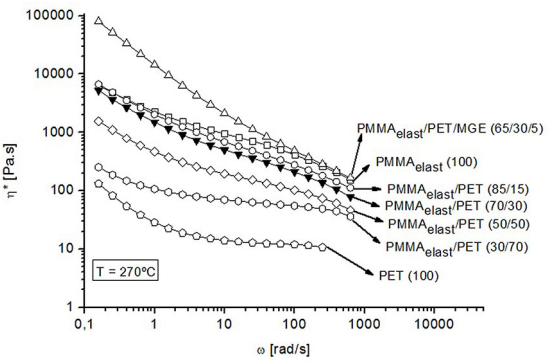

Figure 7. Complex viscosity (η*) vs. frequency (ω) of the pure polymers and the PMMA$_{elast}$/PET and PMMA$_{elast}$/PET/MGE blends at 270ºC.

4. Conclusions

This microrheological study of PMMA$_{elast}$/PET binary blend and PMMA$_{elast}$/PET/MGE compatibilized blend was possible through the use of parallel plates rheometry in dynamic-oscillatory mode and atomic force microscopy (AFM). Based on low shear rate rheology, a study was made of the storage modulus as a function of the loss modulus and the complex viscosity of the pure polymers, the binary blend up to phase inversion and compatibilized blend. The use of sample preparation by cryo-ultramicrotomy enabled the study of the PMMA/PET interface by atomic force microscopy.

5. Acknowledgments

The authors gratefully acknowledge the financial support of the Brazilian research funding agencies CAPES (Federal Agency for the Support and Improvement of Higher Education), CNPq (National Council for Scientific and Technological Development) and FINEP (Research and Projects Financing Agency). We also thank the company UNIGEL S.A. for donating the PMMA used in this study.

6. References

1. Mallete JG, Márquez A, Manero O, Castro-Rodríguez R. Carbon black filled PET/PMMA Blends: electrical and morphological studies. *Polymer Engineering & Science*. 2000;40(10):2272-2278.

2. Dewangan B, Jagtap RN. Amphiphilic block copolymers of PtBA-b-PMMA as compatibilizers for blends of PET and PMMA. *Polymer Engineering & Science*. 2006;46(9):1147-1152.

3. Al-Mulla A. Isothernal crystallization kinetics of poly(ethylene terephtalate) and poly(methyl methacrylate) blends. *Express Polymer Letters*. 2007;1(6):334-344.

4. Al-Salem SM, Khan AR. On the degradation kinetics of poly(ethylene terephthalate) (PET)/poly(methyl methacrylate) (PMMA) blends in dynamic thermogravimetry. *Polymer Degradation and Stability*. 2014;104:28-32.

5. Utracki LA. Compatibilization of polymer blends. *The Canadian Journal of Chemical Engineering*. 2002;80(6):1008-1016.

6. Koning C, Van Duin M, Pagnoulle C, Jerome R. Strategies for compatibilization of polymer blends. *Progress in Polymer Science*. 1998;23(4):707-757.

7. Sung YT, Han MS, Hyun JC, Kim WN, Lee HS. Rheological properties and interfacial tension of polypropylene-poly(styrene-co-acrylonitrile) blend containing compatibilizer. *Polymer*. 2003;44(5):1681-1687.

8. Hale W, Keskkula H, Paul DR. Compatibilization of PBT/ABS blends by methyl methacrylate-glycidyl methacrylate-ethyl acrylate terpolymers. *Polymer*. 1999;40(2):365-377.

9. Larocca NM, Ito EN, Rios CT, Pessan LA, Bretas RES, Hage E Jr. Effect of PBT molecular weight and reactive compatibilization on the dispersed-phase coalescence of PBT/SAN blends. *Journal of Polymer Science Part B: Polymer Physics*. 2010;48(21):2274-2287.

10. Larocca NM, Hage E Jr, Pessan LA. Effect of reactive compatibilization on the properties of poly(butylene terephthalate)/acrylonitrile-ethylene-propylene-diene-styrene blends. *Journal of Polymer Science Part B: Polymer Physics*. 2005:43(10):1244-1259.

11. Costa LC, Ternes Neto A, Hage E. PMMA/SAN and SAN/PBT nanoblends obtained by blending extrusion using thermodynamics and microrheogy basis. *eXPRESS Polymer Letters*. 2014;8(3):164-176.

12. Dantas RLF. *Estudo morfológico da blenda polimérica poli(metacrilato de metila)/poli(tereftalato de etileno) reciclado PMMA*/PET. [Dissertação]. Natal: Universidade Federal do Rio Grande do Norte; 2011. 90 p.

13. Pires-de-Souza FCP, Panzeria H, Vieira MA, Garcia LFR, Consani S. Impact and fracture resistance of an experimental acrylic polymer with elastomer in different proportions. *Materials Research*. 2009;12(4):415-418.

14. Reinaldo JS. *Processamento e caracterização da blenda poli(metacrilato de metila) (PMMA) elastomérico e poli(tereftalato de etileno) (PET) pós-consumo* [Dissertação]. Natal: Universidade Federal do Rio Grande do Norte; 2013. 120 p.

15. Mano EB. *Polímeros como Materiais de Engenharia*. São Paulo: Edgard Blucher; 2003.

16. Reinaldo JS, Nascimento MCBC, Ito EN, Hage E Jr. Rheological, mechanical and morphological properties of poly(methyl methacrylate)/poly(ethylene terephthalate) blend with dual reactive interfacial compatibilization. *Polímeros*. 2015;25(5):451-460.

17. Han CD. *Rheology and processing of polymeric materials*. New York: Oxford University Press; 2007.

18. Lee HM, Park OO. Rheology and dynamics of immiscible polymer blends. *Journal of Rheology*. 1994;38(5):1405-1425.

19. Bousmina M, Muller R. Linear viscoelasticity in the melt of impact PMMA. Influence of concentration and aggregation of dispersed rubber particles. *Journal of Rheology*. 1993;37(4):663-679.

20. Hale W, Keskkula H, Paul DR. Fracture behavior of PBT-ABS blends compatibilized by methyl methacrylate-glycidyl methacrylate-ethyl acrylate terpolymers. *Polymer*. 1999;40(12):3353-3365.

21. ASTM International. *ASTM D1238-13 - Standard Test Method for Melt Flow Rates of Thermoplastics by Extrusion Plastometer*. West Conshohocken: ASTM International; 2013.

22. ASTM International. *ASTM D638-10 - Standard Test Method for Tensile Properties of Plastics*. West Conshohocken: ASTM International; 2010.

23. Canevarolo SV Jr. *Técnicas de Caracterização de Polímeros*. 3rd ed. São Paulo: Artliber; 2004.

24. Arruda LC, Magaton M, Bretas RES, Ueki MM. Influence of chain extender on mechanical, thermal and morphological properties of blown films of PLA/PBAT blends. *Polymer Testing*. 2015;43:27-37.

25. Souza AMC, Caldeira CB. An investigation on recycled PET/PP and recycled PET/PP-EP compatibilized blends: Rheological, morphological, and mechanical properties. *Journal of Applied Polymer Science*. 2015;132(17):41892.